

Supplement of Earth Syst. Sci. Data, 11, 1745–1764, 2019  
<https://doi.org/10.5194/essd-11-1745-2019-supplement>  
© Author(s) 2019. This work is distributed under  
the Creative Commons Attribution 4.0 License.



Open Access  
Earth System  
Science  
Data

*Supplement of*

## **The Cumulus And Stratocumulus CloudSat-CALIPSO Dataset (CASC-CAD)**

**Grégory Cesana et al.**

*Correspondence to:* Gregory V. Cesana ([gregory.cesana@columbia.edu](mailto:gregory.cesana@columbia.edu))

The copyright of individual parts of the supplement might differ from the CC BY 4.0 License.

Figure S1: Annual mean profiles (y axis, height [km]) of cloud frequency (x axis) over the Barbados (between 61.5°W and 49.5°W and 11°N and 19°N) for different satellite datasets (colored lines) and for the Barbados Cloud Observatory (Nuijens et al., 2014) with (solid grey line) and without precipitation (dashed grey line). The dash-dot, dash and solid blue lines correspond to CALIPSO Kyushu University (Cesana et al., 2016), CALIPSO Science Team (Cesana et al., 2016) and CALIPSO-GOCCP (Guzman et al., 2017, same as used in this study) datasets. The solid and dash red lines correspond to CloudSat dataset (Marchand et al., 2008) with and without precipitation (following the definition of Nuijens et al., 2014). The solid and solid-circle green lines correspond to RL-GeoProf dataset with (same as used in this study and Cesana et al., 2019b) and without CF<sub>lidar</sub> threshold. Finally, the dash-dot and solid purple lines correspond to an older version of the RL-GeoProf dataset using an erroneous lidar product (Kay and Gettelman, 2009) and the 2BCCL dataset using a different Lidar input from the current RL-GeoProf product. Modified from Nuijens et al. (2014).

### Cloud Frequency over the Barbados (BCO)

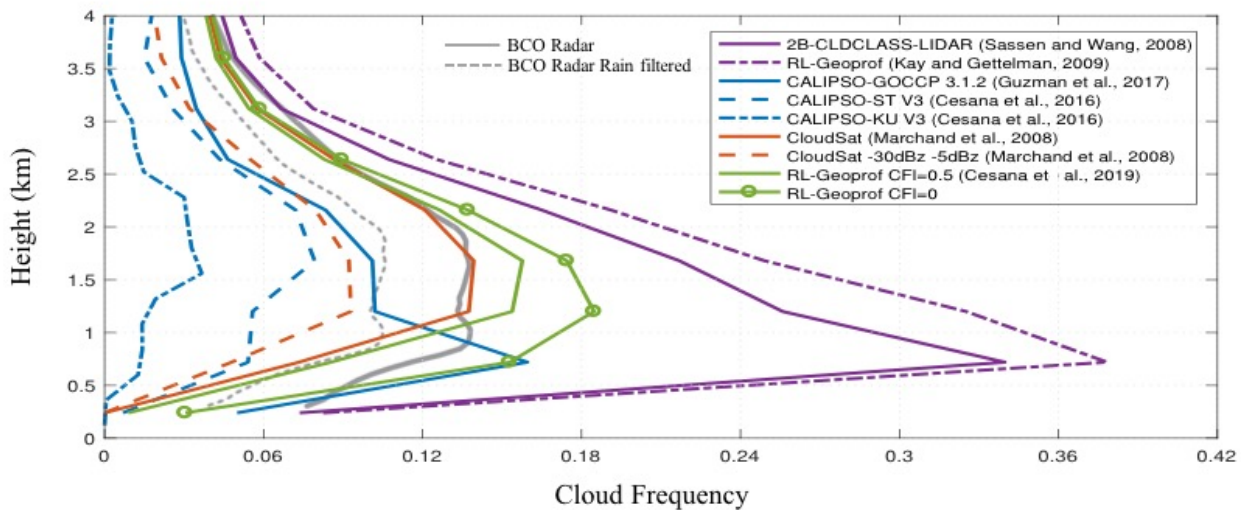


Figure S2: Daytime orbit segment off the coast of California ( $\sim 8^{\circ}\text{N}$  to  $46^{\circ}\text{N}$ , 2008-07-08 21:47:30) showing a typical stratocumulus case for the RL-GeoProf Sc-Cu mask using (a) R04 and (b) R05 product. Reddish and bluish pixels correspond to Sc and Cu type of clouds, respectively. From the top to the bottom, the GOCCP Sc-Cu mask color bar's labels correspond to cumulus, Sc-Cu transitioning, broken Sc, edge of Sc, stratocumulus, and clear pixels.

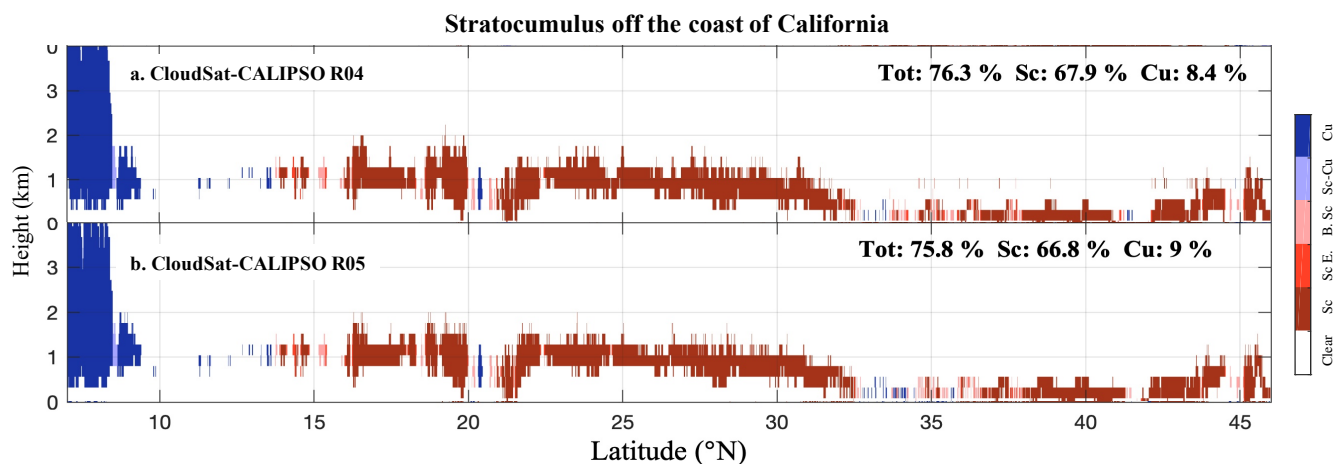


Figure S3: Same as Fig. S2 for a typical cumulus case in the south-east Pacific ( $\sim 37^{\circ}\text{S}$  to  $8^{\circ}\text{S}$ , 2008-07-08 21:47:30, daytime)

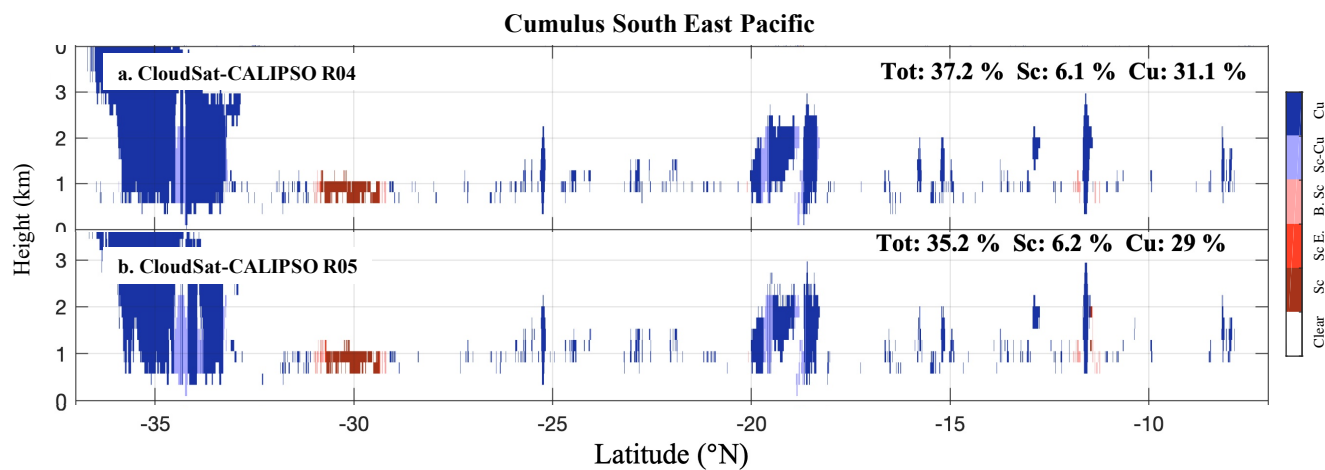
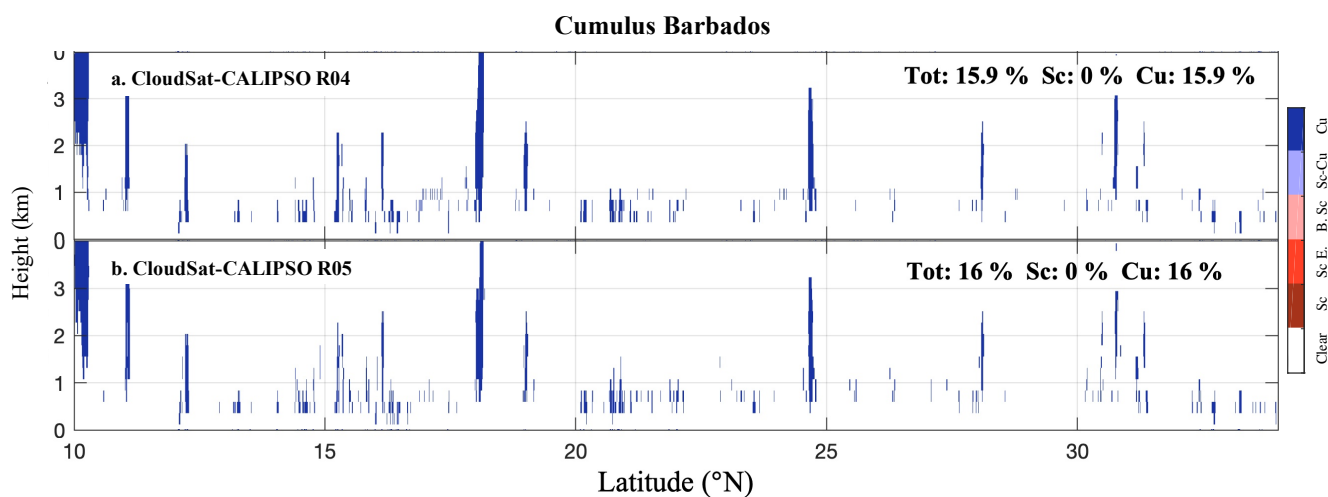


Figure S4: Same as Fig. S2 for a cumulus case overpassing the Barbados (~ 10°N to 35°N, 2008-07-09 17:34:08 daytime).



5 Figure S5: Same as Fig. S2 but for a typical Open-cell Sc to Cu transitioning case overlapping the south-east Pacific and the Southern Ocean (~ 55°S to 20°S, 2008-07-14 21:10:19, daytime).

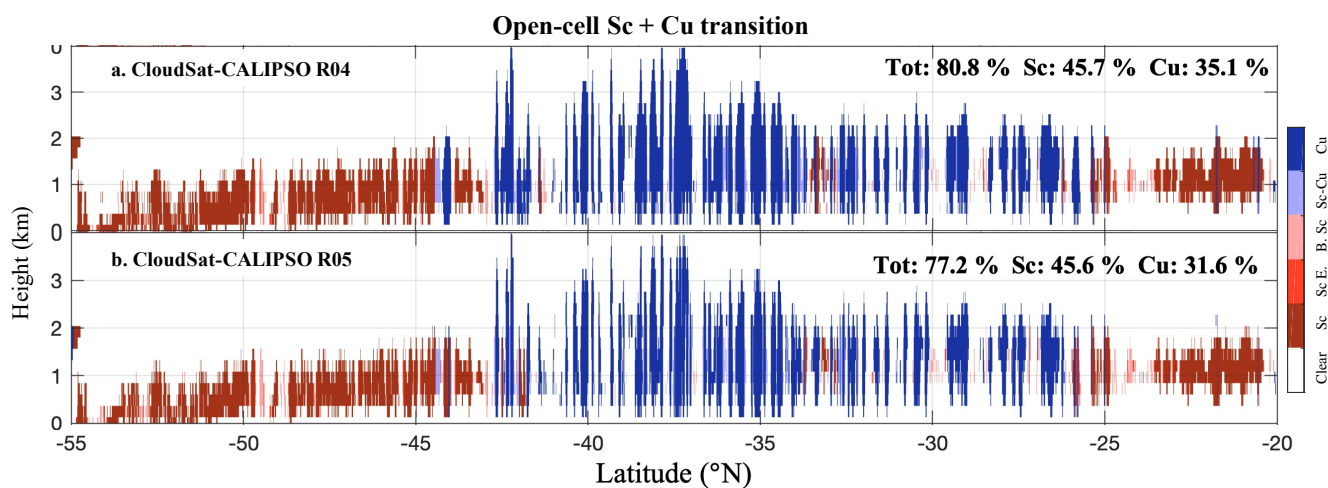
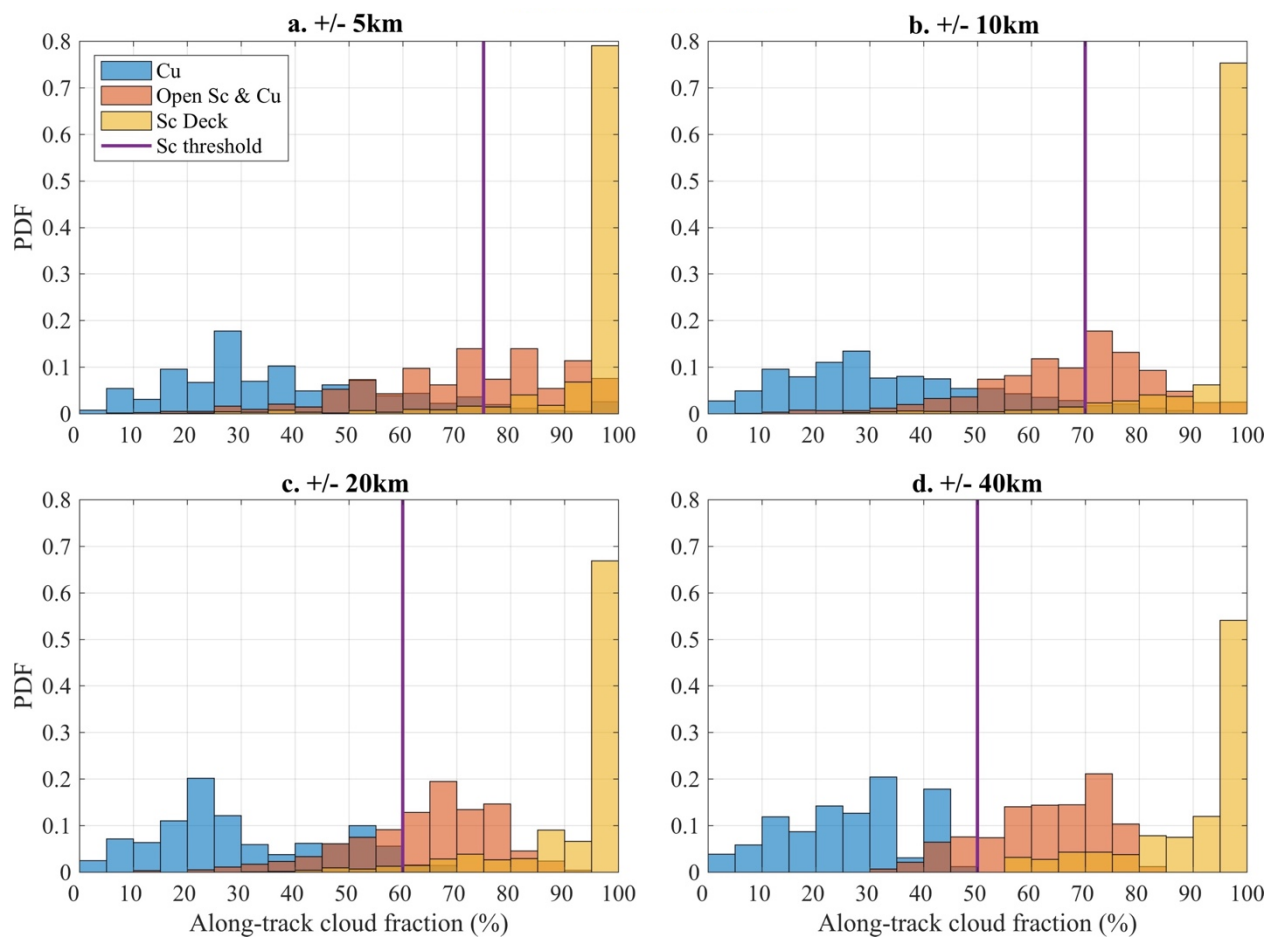


Figure S6: PDF of the different along-track CHCFs for Cu (blue), broken Sc and Sc-Cu transitioning (light red) and Sc (yellow) typical regions computed from eight orbit segments. The thresholds are represented in purple, at approximately the overlap of the Sc and Cu distributions.



5

Figure S7: Map of (x axis, longitude [ $^{\circ}$ E]; y axis, latitude [ $^{\circ}$ N]) of low-level cloud fraction (%) as observed by CALIPSO-GOCCP (2007-2016). All the orbit segments used in the case study analysis (section 4.1) are represented on the map: stratocumulus off the coast of California (in red), the cumulus in the south-east Pacific and near the Barbados (in blue) and the open-cell Sc and Sc-Cu transitioning case between the south-east Pacific and the Southern Ocean (in grey).

5

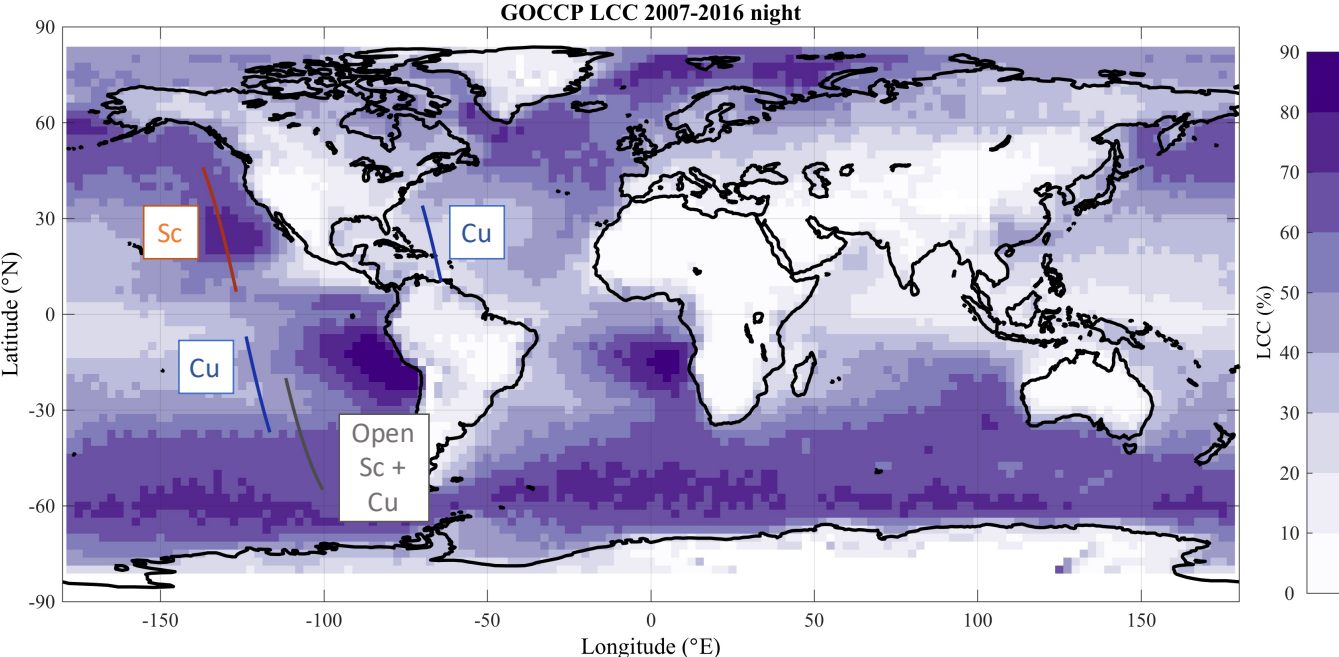


Figure S8: Maps (x axis, longitude [ $^{\circ}$ E]; y axis, latitude [ $^{\circ}$ N]) of (a) the ratio Sc to Sc-and-Cu cloud (%) for GOCCP Sc-Cu mask, (b) the ratio of opaque to opaque-and-thin cloud (%), as defined in Guzman et al., 2017) and (c) the difference between (b) and (c).

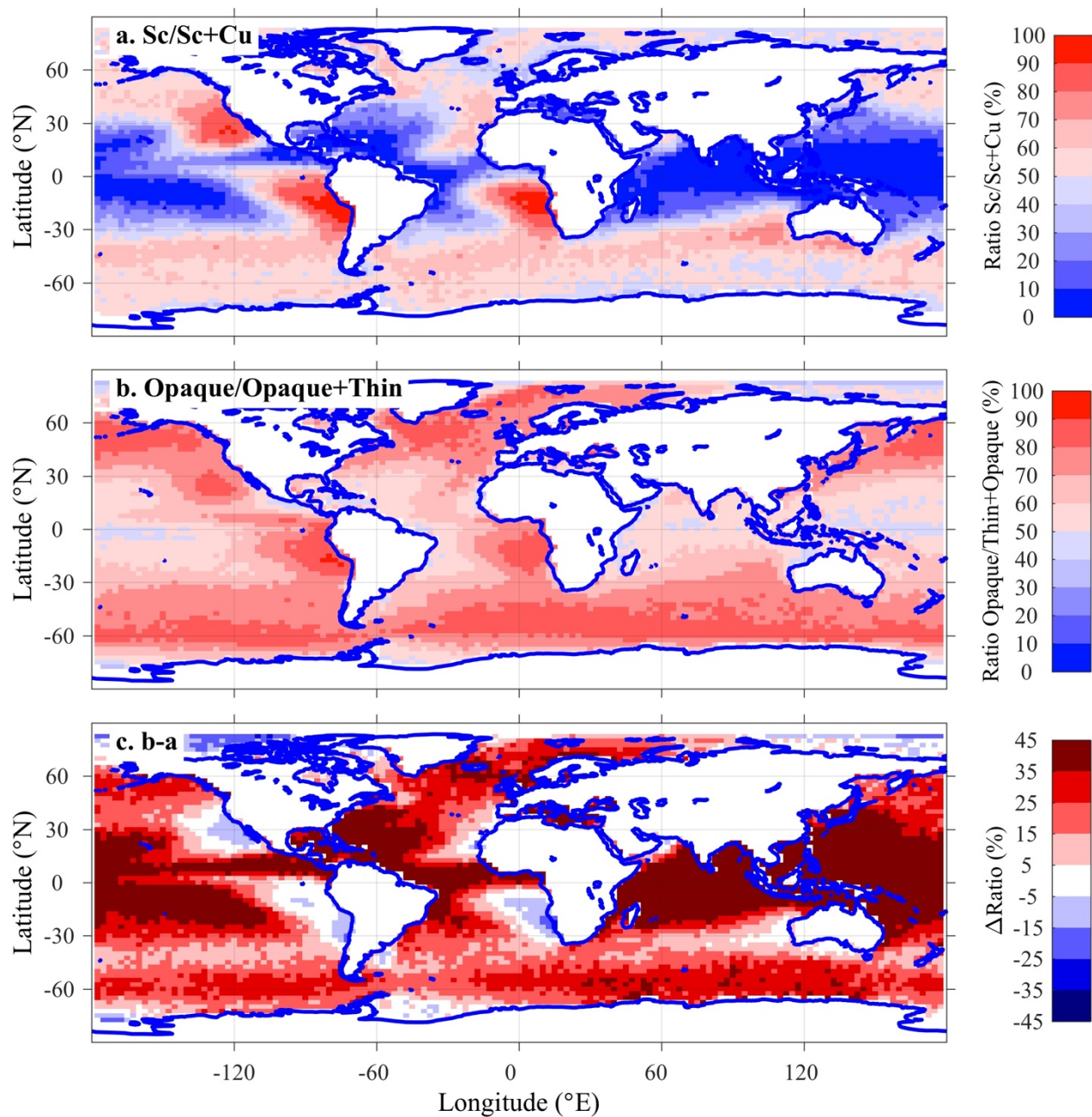
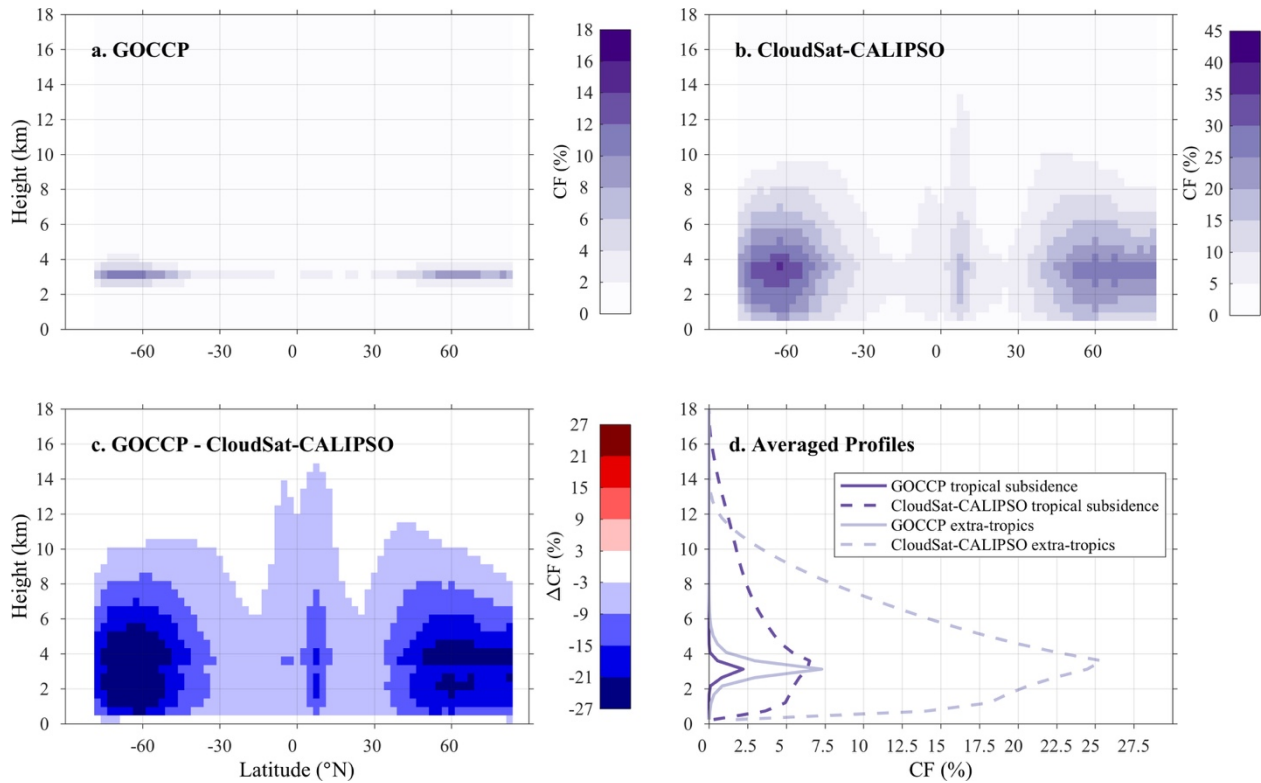


Figure S9: Profiles (y axis, height [km]) of zonally-averaged clouds (x axis, latitude [ $^{\circ}$ N]) with a mid- or high-level cloud top and low-level cloud base –i.e., excluding Sc, Cu and Sc-Cu transitioning clouds– for (a) GOCCP, (b) RL-GeoProf and (c) the difference between (a) and (b). The averaged profiles in tropical subsidence regimes ( $\omega_{500} > 10$  hPa/day between  $35^{\circ}$ S/N, solid line) and in the extra-tropics (poleward  $35^{\circ}$ S/N, dashed lines). The light and dark purple lines in (d) correspond to GOCCP and RL-GeoProf, respectively. In regimes dominated by low clouds, i.e., tropical subsidence regimes, these mid- and high-level topper clouds are very rare and generate only a small difference between GOCCP and RL-GeoProf (d, solid lines) compared to the extra-tropics (d, dashed lines).



10

Figure S10: Profiles (x axis, cloud fraction [%]; y axis, height [km]) of low (first row), Sc (second row), Cu (third row) and Sc-Cu transitioning (fourth row) clouds for (solid line), RL-GeoProf (dashed line) and 2BCCL (dotted line) in tropical subsidence regimes ( $\omega_{500} > 10$  hPa/day between 35°S/N, left column same as Fig. 15, fourth column), at mid-latitudes (between 35°S/N to 60°S/N, middle column) and in the polar regions (poleward 60°, right column).

5

